IN-46-CR
78281
P.15

Global Electric Field Determination in the Earth's Outer Magnetosphere using Charged Particles

FIRST-YEAR PROGRESS REPORT
NASA Guest Investigator Grant NAG5-1558

Principal Investigator:
T. Eastman, Univ. of Maryland
Co-Investigators:
R. Sheldon and D. Hamilton, UMd;
C. McIlwain, UCSD

March 31, 1992

1991 Progress Report

I. Introduction

Although many properties of the Earth's magnetosphere have been measured and quantified in the past 30 years since it was discovered, one fundamental (for a zeroeth order MHD equilibrium) measurement has been made infrequently and with poor spatial coverage: the global electric field. This oversight is in part due to the difficulty of measuring a plasma electric field, and in part due to the neglect of theorists. However there is renewed interest in the convection electric field, since it has been realized that it is vital for understanding many aspects of the magnetosphere: the global MHD equilibrium, reconnection rates, Region 2 Birkeland currents, magnetosphere-ionosphere coupling, ring current and radiation belt transport, substorm injections, acceleration mechanisms, etc. Unfortunately the standard experimental methods have not been able to synthesize a global field (excepting the pioneering work of McIlwain's geostationary models), and we are left with an overly simplistic theoretical field, the Volland-Stern electric field model. Again, single point measurements of the plasmapause were used to infer the appropriate amplitudes of the model, parameterized by Kp [Maynard & Chen, JGR 1975]. Although this result was never intended to be the definitive electric field model, it has gone nearly unchanged for 15 years.

However the data sets being taken today require a great deal more accuracy than can be provided by the Volland-Stern model. Nor has the variability of the electric field shielding been properly addressed, although effects of penetrating magnetospheric electric fields has been seen in mid- and low-latitude ionospheric data sets. The growing interest in substorm dynamics also requires a much better assessment of the electric fields responsible for particle injections. Thus we proposed and developed algorithms for extracting electric fields from particle data taken in the earth's magnetosphere. As a test of the effectiveness of these techniques, we will analyze data taken by the AMPTE/CCE spacecraft in equatorial orbit between 1984-1988. Some analytic tools had to be developed before construction of computer algorithms and we discuss this next.

II. Analytical Tools

To reconstruct the global electric field from single point measurements would require a fleet of spacecraft, which is generally not feasible. The CLUSTER spacecraft(s) to be launched later this decade will address some of these issues, but will not resolve the global character of the electric field from direct measurements. Thus we must rely on a secondary method, namely, using charged particles as tracers of the global fields, with resolution time scales on the order of the convection times, ~hours. While this limits the method somewhat, it provides more than sufficient resolution for correlation with Kp, Dst, hourly AE, solar wind parameters and perhaps some substorm studies. This method has a long history, having been used successfully by McIlwain to analyze geostationary satellite data. Thus we need a robust, efficient, particle tracing method that can be incorporated into an effective algorithm for extracting electric fields from particle data.

The usual approach is to integrate the guiding center equations with a sophisticated ordinary differential equation solver. This brute force method requires extensive CPU time (since the time steps have to be on the order of a gyroperiod) and traces one particle at a time. In order to describe the experimental data, many particles must be traced in order to build up a phase space density spectrum of the convecting particles. Because the final answer is nonanalytic, it is not extensible, parametric, or very predictive. Nor does it lend itself to an "invertible" algorithm for extracting the electric field.

However there is an alternative method that makes use of the adiabatic invariants of the motion. In essence, it is a Hamiltonian, energy conservation approach to the problem in contrast to the Lagrangian, integration of forces approach above.

A. Drift Motion in the Magnetosphere

The key to this approach is found in Whipple's [JGR 1978] work on UB(K) coordinates. For particles mirroring at the equator, and therefore lacking any parallel velocity, the total energy can be written:

$$\text{Tot.E.} = \text{K.E.} + \text{P.E.} = \text{mu B} + \text{q U}$$

where mu is the first adiabatic invariant, B is the magnitude of the magnetic field, q is the particle charge state, and U is the electrostatic potential. Then tracing a particle's trajectory is merely finding the constant energy contours in the equatorial plane. The insight from Whipple, is that this same method works equally well for particles not mirroring at the equator, as long as we replace B with Bm, the mirror point B magnitude. Since Bm is not a conserved quantity of particle motion, but the second adiabatic invariant, J, or its relative K=J/SQRT(2 m mu) is conserved, if dB/dt=0, our task is to find the dependence of Bm(K), and we can now trace the drift motion for any pitch angle, any energy particle through the magnetosphere.

A corollary to this approach arises from the invariance of three of the quantities in the above equation. Thus taking deriviatives gives the relation,

$$dU/dB(K) = -mu/q.$$

That is, if we transform our coordinates to U-B(K) space, the particle trajectories become straight lines, whose slope depends only on their magnetic moment and charge. This coordinate space greatly simplifies our computer algorithm and furthers our intuition.

In implementing the B(K) mapping, we discovered that we had to define a more robust definition of K that would be defined on field lines with multiple minima. If we define a new K (and J) to be the sum over all trapped particle populations separated by possible intervening maxima on the field line, we recover a well behaved invariant for all field lines. This definition can be validated by testing for conservation of the total energy of the convecting particles which maintain this new invariant.

A second corollary arises from the recognition that although U-B(K) space is two dimensional, the particles travel in essentially one dimension. The other dimension must then be identified with diffusion. (Since diffusion along the convection direction is essentially diffusion in drift phase, and since this information is lost in most steady state models, we retain only the perpendicular component.) Note that this diffusion entails no change in mu or K, maintaining the adiabatic invariants and thus the validity of the Hamiltonian approach. This provides a powerful way to disentangle the effects of convection from the effects of diffusion, and thus resolve some of the inconsistencies in the standard diffusion model as found by Lyons and Schulz [JGR 1989].

B. Phase space density evolution

The second key to our approach is quantifying the effect of convection on the phase space density. This was first described by Wolf [Solar Terrestrial Physics, 1983] but only for equatorially mirroring particles. We generalize and rederive his result for all pitch angles. The reduced Vlasov equation integrated over gyrophase and bounce phase (or enhanced continuity equation) can be written:

$$df(mu,K)/dt + div(v\ f(mu,K)) = [\text{charge exchange losses} + \text{diffusion} + \text{Coulomb drag}]$$

The second term becomes:

$$\text{div}(f(\mu,K)) = f(\mu,K)\ \text{div}(v) + v\ \text{grad}(f(\mu,K))$$

Using Whipple's derivation of the drift velocity on a constant K-surface:

$$\text{div}(v) = -v\ \text{grad}(B\ \text{grad}(K))/(B\ \text{grad}(K))$$

Finally, combining this into the original equation, and dividing by f gives:

$$d(\ln(f))/dt + v\ \text{grad}(\ln(f/(B\ \text{grad}(K)))) = [\text{charge exchange rate} + \text{diffusion}/f + C\ d(\ln(f))/d(\mu)]$$

This master equation is very powerful. If we have a steady state solution, so that the first term is zero, and if we neglect the right hand side, then the quantity f/(B grad(K)) remains constant along a drift trajectory. If the particles drift into a region of stronger B, they will also adiabatically have increased density as well. We now have the tools to describe the algorithm below.

III. Inversion Algorithm

The algorithm begins with a data set of measured phase space densities that can be binned in magnetospheric coordinates, preferably with measurements of the local magnetic field.

1) The phase space densities are normalized by dividing by (B grad(K)), where we have used an appropriate model for K.

2) We then choose a particular model for U, and plot the data in U-B(K) space. We want iso-f_density contours to be straight lines, indicating we have a good choice for U and B. This is most obvious at the boundary between convecting and diffusing ions. The use of different mu and K values enables us to map this boundary at many different points in the magnetosphere.

3) The "blur" at this boundary also tells us something about the diffusion rate, which in turn is related to the perturbation electric field. So in addition to a DC electric field, we also get an estimate of the power in the AC field in the appropriate frequency range.

We expect the method to be iterative for U and B, although we will probably not try to modify the B models used.

IV. Progress

Currently we have completed a B(K) tracing package that can find the mirror point magnetic field given an arbitrary magnetic field model (Tsyganenko 89 or Olson-Pfitzer 88 for example). We have incorporated several electric field models that include an ionospheric field as found by Richmond et al. [1980]. With this combination, we have traced trajectories through the magnetosphere for arbitrary pitch angle (see Figure 1), and noted some features that may explain some puzzling observations from ISEE [Williams and Frank, 1982]. In a qualitative UB(K) analysis of AMPTE/CCE/CHEM quiet time data set, we show the dominance of the ionospheric field below L=3, both in DC and AC components (Figure 2). These results have been presented at AGU's Spring meeting, and will be submitted to JGR.

Our next task is to construct a package using a maximum likelihood estimator of "goodness of fit" to compare data with the model. This will provide the iterative portion of the fitting between models and data. We estimate that this will take between 6 months and a year to complete. With this in hand, we will then analyze as much of the AMPTE/CCE/CHEM data as possible to construct a statistical data base of electric fields for the eventual improvement of the Maynard-Chen relation. These algorithms will also be of value for the ISTP era of data analysis.

V. Applications

Beyond the construction of the above algorithm, we envision applying this data set to the following problems:

1) A calculation of the divergence of current at the equator from the actual phase space densities, and comparison with high latitude measurements, AE, Dst etc.

2) A calculation of the evolving phase space distribution with particular care in regions where the distribution is unstable with respect to wave-growth, and in particular, electromagnetic ion cyclotron waves.

3) A correlation of electric fields with estimates of the reconnection rate from upstream monitors of the solar wind.

4) A correlation between electric field and substorm or storm progression, injection events, Dst and aurorae.

5) A correlation of electric field with ionospheric electric field measurements, penetrating electric fields, neutral winds, f0f2, etc. This pushes the maximum time resolution of the method, which in turn depends on the orbit dynamics of the spacecraft used.

6) A correlation of electric fields measured with the 1-100 keV population with measurements of the cold plasmasphere distribution, location of the plasmapause, whistler observations, etc.

VI. Figure Captions

Figure 1. Ion drift trajectories in a realistic field model: Tsyganenko 1989 magnetic field model for Kp=0 with no dipole tilt, Volland-Stern electric field for Kp=0 added to a Richmond et al. 1980 ionospheric electric field. Heaviest curve is a Sibeck et al. 1989 magnetopause at 10.5 Re. Heavier lines are magnetic field equipotentials at dipole field strengths corresponding to 2, 3, ...,12 Re at the equator. Note the greater field strengths for larger K, where K is given in units of Gauss^.5-Re. Thin lines are the constant energy contours which are equivalent to drift trajectories in the equatorial plane. Note the appearance of closed drift paths not encircling the earth near noon at low K, but disappearing for higher K. Dashed lines indicate the location of the tangency between magnetic and electrostatic equipotentials corresponding to the limiting boundaries in U-B(K) space. Note the quadrupolar ionospheric field produces four tangency points at a given radius close to the earth before being swamped by the Volland-Stern field further out. (Wiggles in the tangency curves near dawn are caused by numerical differencing.)

Figure 2. The deepest penetration for convecting ions in a dipole magnetic field and a Volland-Stern electric field is plotted for several values of Kp, (calculated geometrically from the UB(K) representation.) This is superposed on a quiet time data set taken with AMPTE/CCE/CHEM. The color scheme does not Xerox well, but a strong gradient aligns with the high energy edge of the predicted convection boundary. The best fit appears to be with a Kp=1.5. The flux penetrates below the L=3 cutoff predicted by the model however, indicating the need for an ionospheric electric field source. The region to the left of the gradient, at lower mu, is not organized very well by convection boundaries, demonstrating the need for a model that incorporates diffusion, Coulomb drag and charge exchange.

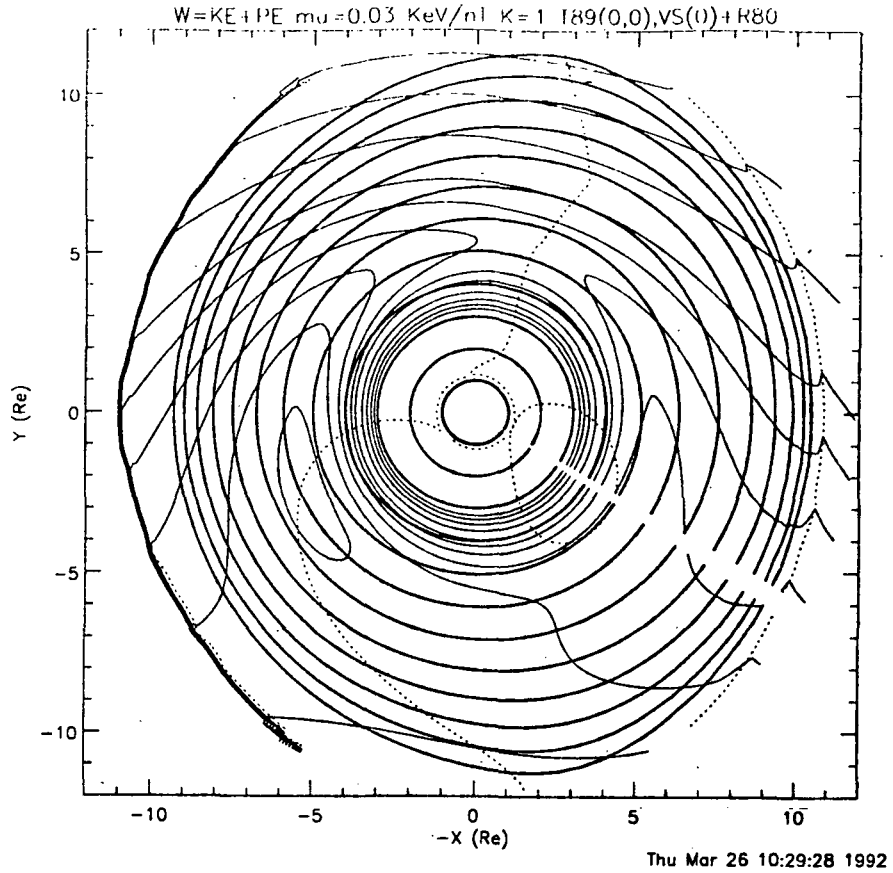
W=KE+PE mu=0.03 KeV/nT K=1 T89(0,0),VS(0)+R80
10
5
0
-5
-10
Y (Re)
-10
-5
0
5
10
-X (Re)
Thu Mar 26 10:29:28 1992

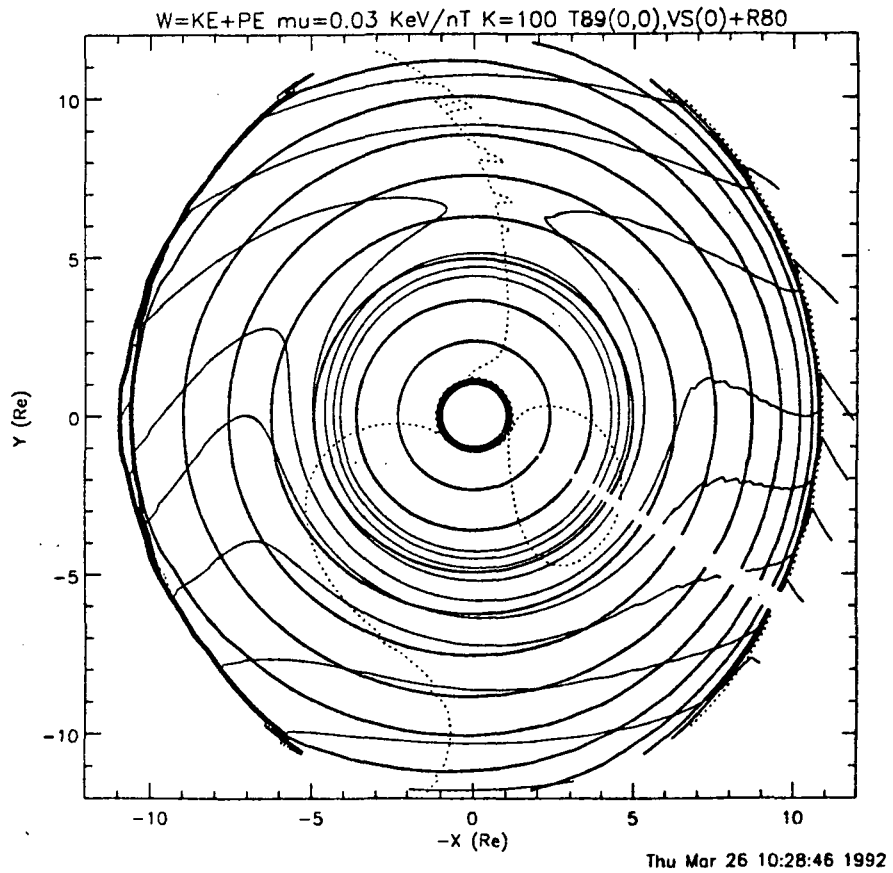
W=KE+PE mu=0.03 KeV/nT K=100 T89(0,0),VS(0)+R80
10
5
0
-5
-10
Y (Re)
-10
-5
0
5
10
-X (Re)
Thu Mar 26 10:28:46 1992

FIGURE 1.

AVERAGE QUIET-TIME PROTONS ($K_p \leq 2$, $|D_{st}| \leq 10$)

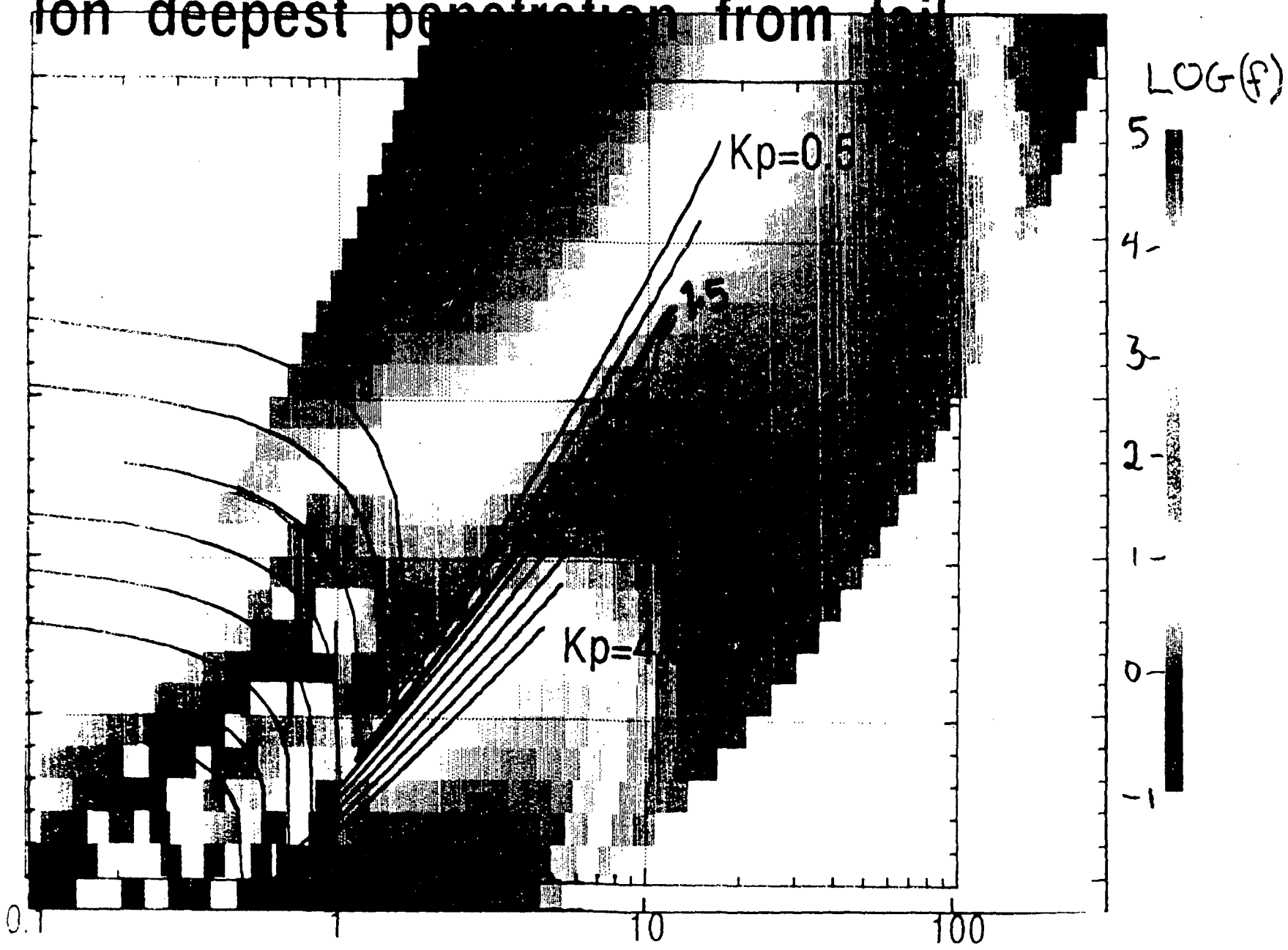

FIG 2.